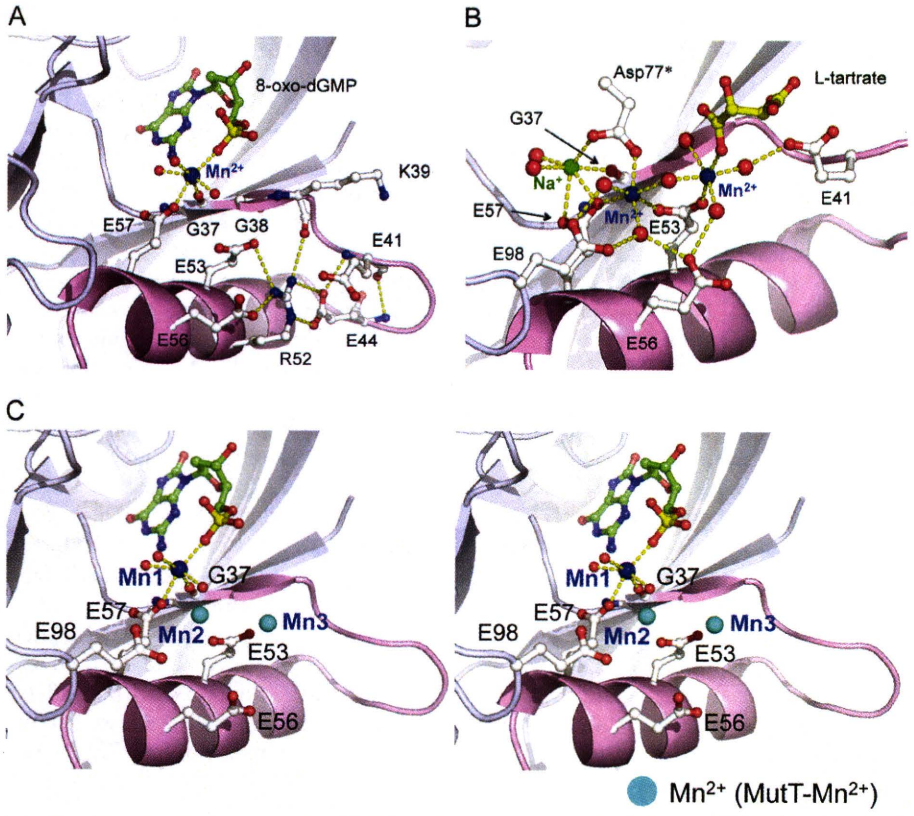

FIGURE 4. **Coordination scheme of Mn^{2+} at the MutT signature in MutT-8-oxo-dGMP-Mn^{2+} and MutT-Mn^{2+}.** *A*, the coordination scheme of Mn^{2+} and the structure of the MutT signature in MutT-8-oxo-dGMP-Mn^{2+}. Mn^{2+} in *blue* has an ideal octahedral coordination with Gly-37, Glu-57, Pα-O of 8-oxo-dGMP, and water molecules. The hydrogen bonding interactions shown in *yellow dashed lines* contribute to the conformational stabilization of the SLHL structure of the MutT signature. The SLHL structure is in *pink*. *B*, the coordination scheme of Mn^{2+} in MutT-Mn^{2+}. Na^+ is shown in *green*. Asp-77* is an amino acid of another molecule in the asymmetric unit. *C*, superposition of two Mn^{2+} ions in MutT-Mn^{2+} onto the structure of MutT-8-oxo-dGMP-Mn^{2+} (*stereo view*). *Coloring* is as in *A*. Mn^{2+} ions observed in MutT-Mn^{2+} are shown in *cyan* (*Mn2* and *Mn3*).

on the preference of the *syn* conformation about the 8-oxoG nucleotides, it is difficult to estimate the free energy difference between the *syn* and *anti* conformations. However, it is unlikely that the preference of MutT for the *syn* conformation over the *anti* conformation is more than 10-fold ($\Delta\Delta G \approx 1.4$ kcal/mol), because the *anti* conformation for 8-oxoG nucleotides is sometimes observed in the crystal structures of 8-oxoG recognition complexes such as OGG1 and MutY (15, 16).

These discrimination factors cannot by themselves explain the roughly 34,000-fold difference between the binding affinity of MutT for 8-oxo-dGMP and dGMP ($\Delta\Delta G \approx 6$ kcal/mol). When 8-oxo-dGMP binds to MutT, large ligand-induced conformational changes with an ordering of loop regions are observed. On the other hand, in the binding of dGMP to MutT, the thermal parameters were $\Delta G = -3.7$, $\Delta H = -3.3$, and $-T\Delta S = -0.4$ kcal/mol; the changes in backbone ^{15}N and NH chemical shifts in 22 residues; and the slowing down of the NH exchange with D_2O of 20 residues are remarkably different when compared with the changes (the thermal parameters of $\Delta G = -9.8$, $\Delta H = -39.0$, and $-T\Delta S = 29.2$ kcal/mol; the changes in backbone ^{15}N and NH chemical shifts in 62 residues; and the slowing down of the NH exchange with D_2O of 45 residues) involved in the binding of 8-oxo-dGMP to MutT (19, 45). These facts suggest that no significant conformational change in MutT is observed when dGMP binds to MutT. The large ligand-induced conformational change in MutT also contributes to the discrimination of 8-oxoG nucleotides from G nucleotides.

A comparison of the amino acid sequences of MutT-related enzymes suggests that the enzymes with higher substrate specificity for 8-oxoG are only MutT homologs from closely related species with conserved amino acids in the positions that participate in the recognition of 8-oxoG and the conformational change (Fig. 1, *green asterisk*). In fact, these amino acids are not highly conserved among *E. coli* Orf135 (51), *Bacillus subtilis* YtkD (52), and hMTH1 (8) that have broad substrate specificities.

Structure of the MutT Signature and Metal-binding Sites—We have solved two types of Mn^{2+}-bound structures, MutT-8-oxo-dGMP-Mn^{2+} and MutT-Mn^{2+}, to determine metal-binding sites at the MutT signature of MutT. The crystal of MutT-Mn^{2+} contains two proteins per asymmetric unit. Their overall structures are very similar, with an r.m.s.d. of 0.3 Å for the corresponding 118 Cα atoms; for simplicity, only one molecule will be referred to in all further discussion. The structure of MutT-Mn^{2+} is similar to that of the apo form, with an r.m.s.d. of 0.6 Å for the corresponding 118 Cα atoms.

In the MutT signature having an SLHL structure (Fig. 4*A*), Gly-38, Glu-44, Arg-52, Glu-53, Glu-56, Glu-57, and Gly-59 are completely conserved among the members of the Nudix family (Fig. 1). The SLHL structure of MutT is similar to those of other enzymes in the Nudix family. For example, the conserved 23 residues can be superimposed on those found in the *Pyrobaculum aerophilum* Nudix protein with an r.m.s.d. of 0.5 Å (53). A characteristic feature in the SLHL structure is the hydrogen-bonding network centering on the converged Arg-52 that anchors α-1 to its connecting loop. The side chains of Glu-44 and Arg-52, which form two hydrogen bonds with each other, participate in hydrogen bonding to the main chain atoms in the nonconserved Glu-41 and Lys-39 residues, respectively. Arg-52 also interacts with the side chains of the conserved Glu-53 and Glu-56 residues (Fig. 4*A*). This hydrogen-bonding network is roughly the same as that in the other Nudix proteins and contributes to the conformational stability of the SLHL structure (39, 40, 53–65).

In the electron density maps of the MutT-Mn^{2+} crystal produced by co-crystallization, there were three peaks corresponding to the metal ions near the MutT signature. Judging from the peak heights, *B* factors, bond lengths, and bond angles, we determined that two peaks were Mn^{2+} ions (nearly ideal octahedral coordination and an average bond length of ~2.2 Å) and one was Na^+ (distorted octahedral coordination and an average bond length of ~2.5 Å) (Fig. 4*B*). Furthermore, the two Mn^{2+} sites were also confirmed from significant densities (>10 σ level) on the anomalous difference Fourier map at $\lambda = 1$ Å (data not shown). On the other hand, the densities of the Na^+ site were less than noise level. The refined MutT-Mn^{2+} structure reveals that two Mn^{2+} ions form a binuclear metal center with a bridged water molecule. One Mn^{2+} coordinates to the oxygen atoms of Glu-53, Glu-57, three water molecules, and Asp-77 in another molecule (Asp-77*). The coordination partners of another Mn^{2+} are Glu-53, L-tartrate (a crystallization reagent), and four water molecules. Na^+ coordinates to the oxygen atoms of Gly-37, Glu-57, Asp-77*, and two water molecules. Asp-77* and L-tartrate bind to the MutT signature through metal ions, but do not distort the SLHL structure.

In the MutT-8-oxo-dGMP-Mn^{2+} crystal (prepared by soaking MutT-8-oxo-dGMP crystals in reservoir supplemented with 1 mM $MnCl_2$), Mn^{2+} binds to the six oxygen atoms of the main chain of Gly-37, the side chain of Glu-57, the phosphate group, and three water molecules with nearly ideal octahedral coordination (Fig. 4*A*). The binding of Mn^{2+} to the MutT-8-oxo-dGMP binary complex makes the phosphate group move slightly toward Mn^{2+} (the P atom moves by 0.7 Å). The position of Mn^{2+} observed in MutT-8-oxo-dGMP-Mn^{2+} is close to that of Na^+ in MutT-Mn^{2+} (at a distance of 1.4 Å). The three Mn^{2+} binding sites consisting of the Mn^{2+} in MutT-8-oxo-dGMP-Mn^{2+} and two additional Mn^{2+} ions in MutT-Mn^{2+} (Fig. 4*C*) are located at common metal-binding sites observed in the Nudix family (60) and correspond to those observed in the ternary complexes of *E. coli* ADP-ribose pyrophosphatase, *Mycobacterium tuberculosis* ADP-ribose pyrophosphatase, *Caenorhabditis elegans* diadenosine 5′,5‴-P^1,P^4-tetraphosphate pyrophosphohydrolase, *Xenopus laevis* X29, human NUDT5, *Thermus thermophilus* Ndx2, and BdRppH (40, 55, 57, 64–67). Thus, the three sites are considered to be candidates for metal binding in 8-oxo-dGTP hydrolysis. Previous kinetic studies have shown that MutT binds to one Mn^{2+} in the absence of nucleotides and two Mn^{2+} ions in the presence of a nonspecific substrate analog, AMPCPP (68). The middle Mn^{2+} (*Mn2* in Fig. 4*C*) may be prebound to the active site, judging from the number of coordination partners in MutT and the Mn^{2+} ion (*Mn1* in Fig. 4*C*) found in MutT-8-oxo-dGMP-Mn^{2+}; otherwise, it and other Mn^{2+} ion (*Mn1* and *Mn3*, respectively in Fig. 4*C*) would be recruited with the substrate. The probability of the three metals binding to MutT in the presence of the real substrate 8-oxo-dGTP cannot be neglected because of the fact that the number of binding metals depends on the kinds of substrate analogs (40, 54, 60, 61, 64–66).

The structures of MutT-8-oxo-dGMP-Mn^{2+} and MutT-Mn^{2+} suggest structural insights into some essential or important residues for the 8-oxo-dGTP hydrolysis. Glu-53 and Glu-57 are essential for the suppression of spontaneous A:T to C:G transversion mutations (69), and E53Q and E57Q mutants decrease k_{cat} by 10^4 to 10^5-fold (70). On the other hand, Glu-56 is nonessential for the suppression of the mutations (69), and E56Q and E98Q mutants have relatively small effects (<24-fold) on k_{cat} (70). These results agree with our structural studies showing that essential residues, Glu-53 and Glu-57, directly bind to metal ions, whereas important residues, Glu-56 and Glu98, make water-mediated interactions with metal ions (Fig. 4, *A* and *B*). Gly-37 and Gly-38, which are located at the surface of the ligand-binding site, are also revealed to be essential residues for the suppression of the mutations (69). The side chains of any residues except Gly in positions 37 and 38 would contact the base moiety of the nucleotide ligand and the essential residue for the catalysis, Glu-53, respectively (Fig. 4, *A* and *C*). For this reason, to express 8-oxo-dGTPase activity, residues 37 and 38 must be Gly, which has the smallest side chain.

A number of kinetic, mutational, and NMR studies of MutT using dGTP and/or a substrate analog, AMPCPP, have been reported, and a catalytic mechanism is proposed by Mildvan and coworkers (71). Compared with our structural data, there appear to be some differences in the metal-binding sites. Gly-38 is involved in metal coordination in their model, but Gly-37, instead of Gly-38, is a metal ligand in the structure of MutT-8-oxo-dGMP-Mn^{2+} (Fig. 4, *A* and *C*). The all-crystal structures of Nudix proteins show that the carbonyl oxygen of the corresponding residue to Gly-38 participates in the formation of β-sheet, whereas that of Gly-37 binds to a metal ion (40, 55, 57–59, 61, 64–67). Glu-56 and Glu98, which are metal ligands in the model proposed by Mildvan and coworkers, interact with water molecules bound to metal ions in our structures. The metal coordination scheme changes in the active site during the reaction, and a more proper enzymatic mechanism activated by metal ions might be examined by kinetic protein crystallography.

REFERENCES

1. Maki, H., and Sekiguchi, M. (1992) *Nature* **355,** 273–275
2. Taddei, F., Hayakawa, H., Bouton, M., Cirinesi, A., Matic, I., Sekiguchi, M., and Radman, M. (1997) *Science* **278,** 128–130
3. Au, K. G., Cabrera, M., Miller, J. H., and Modrich, P. (1988) *Proc. Natl. Acad. Sci. U.S.A.* **85,** 9163–9166
4. Cabrera, M., Nghiem, Y., and Miller, J. H. (1988) *J. Bacteriol.* **170,** 5405–5407
5. Michaels, M. L., Cruz, C., Grollman, A. P., and Miller, J. H. (1992) *Proc. Natl. Acad. Sci. U.S.A.* **89,** 7022–7025
6. Tchou, J., Kasai, H., Shibutani, S., Chung, M. H., Laval, J., Grollman, A. P., and Nishimura, S. (1991) *Proc. Natl. Acad. Sci. U.S.A.* **88,** 4690–4694
7. Ito, R., Hayakawa, H., Sekiguchi, M., and Ishibashi, T. (2005) *Biochemistry* **44,** 6670–6674
8. Fujikawa, K., Kamiya, H., Yakushiji, H., Fujii, Y., Nakabeppu, Y., and Kasai, H. (1999) *J. Biol. Chem.* **274,** 18201–18205
9. Fujikawa, K., Kamiya, H., Yakushiji, H., Nakabeppu, Y., and Kasai, H. (2001) *Nucleic Acids Res.* **29,** 449–454
10. Mishima, M., Sakai, Y., Itoh, N., Kamiya, H., Furuichi, M., Takahashi, M., Yamagata, Y., Iwai, S., Nakabeppu, Y., and Shirakawa, M. (2004) *J. Biol. Chem.* **279,** 33806–33815
11. Tchou, J., Bodepudi, V., Shibutani, S., Antoshechkin, I., Miller, J., Grollman, A. P., and Johnson, F. (1994) *J. Biol. Chem.* **269,** 15318–15324
12. Hatahet, Z., Kow, Y. W., Purmal, A. A., Cunningham, R. P., and Wallace, S. S. (1994) *J. Biol. Chem.* **269,** 18814–18820
13. Fromme, J. C., and Verdine, G. L. (2003) *J. Biol. Chem.* **278,** 51543–51548
14. Porello, S. L., Leyes, A. E., and David, S. S. (1998) *Biochemistry* **37,**

14756–14764
15. Bruner, S. D., Norman, D. P., and Verdine, G. L. (2000) *Nature* **403,** 859–866
16. Fromme, J. C., Banerjee, A., Huang, S. J., and Verdine, G. L. (2004) *Nature* **427,** 652–656
17. Bessman, M. J., Frick, D. N., and O'Handley, S. F. (1996) *J. Biol. Chem.* **271,** 25059–25062
18. Abeygunawardana, C., Weber, D. J., Gittis, A. G., Frick, D. N., Lin, J., Miller, A. F., Bessman, M. J., and Mildvan, A. S. (1995) *Biochemistry* **34,** 14997–15005
19. Massiah, M. A., Saraswat, V., Azurmendi, H. F., and Mildvan, A. S. (2003) *Biochemistry* **42,** 10140–10154
20. Doublié, S. (1997) *Methods Enzymol.* **276,** 523–530
21. LeMaster, D. M., and Richards, F. M. (1985) *Biochemistry* **24,** 7263–7268
22. Nakamura, T., Kitaguchi, Y., Miyazawa, M., Kamiya, H., Toma, S., Ikemizu, S., Shirakawa, M., Nakabeppu, Y., and Yamagata, Y. (2006) *Acta Crystallogr. Sect. F Struct. Biol. Cryst. Commun.* **62,** 1283–1285
23. Akiyama, M., Maki, H., Sekiguchi, M., and Horiuchi, T. (1989) *Proc. Natl. Acad. Sci. U.S.A.* **86,** 3949–3952
24. Nakamura, T., Doi, T., Sekiguchi, M., and Yamagata, Y. (2004) *Acta Crystallogr. D Biol. Crystallogr.* **60,** 1641–1643
25. Rossmann, M. G., and van Beek, C. G. (1999) *Acta Crystallogr. D Biol. Crystallogr.* **55,** 1631–1640
26. Otwinowski, Z., and Minor, W. (1997) *Methods Enzymol.* **276,** 307–326
27. Matthews, B. W. (1968) *J. Mol. Biol.* **33,** 491–497
28. Terwilliger, T. C., and Berendzen, J. (1999) *Acta Crystallogr. D Biol. Crystallogr.* **55,** 849–861
29. Collaborative Computational Project, Number 4. (1994) *Acta Crystallogr. D Biol. Crystallogr.* **50,** 760–763
30. Cowtan, K. (1994) *Joint CCP4 and ESF-EACBM Newsletter on Protein Crystallography* **31,** 34–38
31. Cambillau, C., Horjales, E., and Jones, T. A. (1984) *J. Mol. Graph.* **2,** 53–54
32. Jones, T. A., Zou, J. Y., Cowan, S. W., and Kjeldgaard, M. (1991) *Acta Crystallogr. Sect. A* **47,** 110–119
33. Brünger, A. T. (1992) *A System for X-Ray Crystallography and NMR,* Yale University Press, New Haven, CT
34. Brünger, A. T., Adams, P. D., Clore, G. M., DeLano, W. L., Gros, P., Grosse-Kunstleve, R. W., Jiang, J. S., Kuszewski, J., Nilges, M., Pannu, N. S., Read, R. J., Rice, L. M., Simonson, T., and Warren, G. L. (1998) *Acta Crystallogr. D Biol. Crystallogr.* **54,** 905–921
35. Navaza, J. (1994) *Acta Crystallogr. Sect. A* **50,** 157–163
36. Laskowski, R. A., MacArthur, M. W., Moss, D. S., and Thornton, J. M. (1993) *J. Appl. Crystallogr.* **26,** 283–291
37. Kabsch, W. (1976) *Acta Crystallogr. Sect. A* **32,** 922–923
38. DeLano, W. L. (2002) *The PyMOL Molecular Graphics System,* DeLano Scientific LLC, San Carlos, CA
39. Gabelli, S. B., Bianchet, M. A., Xu, W., Dunn, C. A., Niu, Z. D., Amzel, L. M., and Bessman, M. J. (2007) *Structure* **15,** 1014–1022
40. Messing, S. A., Gabelli, S. B., Liu, Q., Celesnik, H., Belasco, J. G., Piñeiro, S. A., and Amzel, L. M. (2009) *Structure* **17,** 472–481
41. Holm, L., Kääriäinen, S., Rosenström, P., and Schenkel, A. (2008) *Bioinformatics* **24,** 2780–2781
42. Bhatnagar, S. K., Bullions, L. C., and Bessman, M. J. (1991) *J. Biol. Chem.* **266,** 9050–9054
43. Saenger, W. (1984) *Principles of Nucleic Acid Structure,* Springer-Verlag, New York
44. Steyert, S. R., Messing, S. A., Amzel, L. M., Gabelli, S. B., and Piñeiro, S. A. (2008) *J. Bacteriol.* **190,** 8215–8219
45. Saraswat, V., Massiah, M. A., Lopez, G., Amzel, L. M., and Mildvan, A. S. (2002) *Biochemistry* **41,** 15566–15577
46. Saraswat, V., Azurmendi, H. F., and Mildvan, A. S. (2004) *Biochemistry* **43,** 3404–3414
47. Funahashi, J., Takano, K., Yamagata, Y., and Yutani, K. (2002) *J. Biol. Chem.* **277,** 21792–21800
48. Takano, K., Yamagata, Y., Funahashi, J., Hioki, Y., Kuramitsu, S., and Yutani, K. (1999) *Biochemistry* **38,** 12698–12708
49. Kouchakdjian, M., Bodepudi, V., Shibutani, S., Eisenberg, M., Johnson, F., Grollman, A. P., and Patel, D. J. (1991) *Biochemistry* **30,** 1403–1412
50. Uesugi, S., Yano, J., Yano, E., and Ikehara, M. (1977) *J. Am. Chem. Soc.* **99,** 2313–2323
51. Kamiya, H., Murata-Kamiya, N., Iida, E., and Harashima, H. (2001) *Biochem. Biophys. Res. Commun.* **288,** 499–502
52. Xu, W., Jones, C. R., Dunn, C. A., and Bessman, M. J. (2004) *J. Bacteriol.* **186,** 8380–8384
53. Wang, S., Mura, C., Sawaya, M. R., Cascio, D., and Eisenberg, D. (2002) *Acta Crystallogr. D Biol. Crystallogr.* **58,** 571–578
54. Gabelli, S. B., Bianchet, M. A., Bessman, M. J., and Amzel, L. M. (2001) *Nat. Struct. Biol.* **8,** 467–472
55. Bailey, S., Sedelnikova, S. E., Blackburn, G. M., Abdelghany, H. M., Baker, P. J., McLennan, A. G., and Rafferty, J. B. (2002) *Structure* **10,** 589–600
56. Kang, L. W., Gabelli, S. B., Bianchet, M. A., Xu, W. L., Bessman, M. J., and Amzel, L. M. (2003) *J. Bacteriol.* **185,** 4110–4118
57. Kang, L. W., Gabelli, S. B., Cunningham, J. E., O'Handley, S. F., and Amzel, L. M. (2003) *Structure* **11,** 1015–1023
58. Shen, B. W., Perraud, A. L., Scharenberg, A., and Stoddard, B. L. (2003) *J. Mol. Biol.* **332,** 385–398
59. Gabelli, S. B., Bianchet, M. A., Azurmendi, H. F., Xia, Z., Sarawat, V., Mildvan, A. S., and Amzel, L. M. (2004) *Structure* **12,** 927–935
60. Ranatunga, W., Hill, E. E., Mooster, J. L., Holbrook, E. L., Schulze-Gahmen, U., Xu, W., Bessman, M. J., Brenner, S. E., and Holbrook, S. R. (2004) *J. Mol. Biol.* **339,** 103–116
61. Yoshiba, S., Ooga, T., Nakagawa, N., Shibata, T., Inoue, Y., Yokoyama, S., Kuramitsu, S., and Masui, R. (2004) *J. Biol. Chem.* **279,** 37163–37174
62. She, M., Decker, C. J., Chen, N., Tumati, S., Parker, R., and Song, H. (2006) *Nat. Struct. Mol. Biol.* **13,** 63–70
63. Zha, M., Zhong, C., Peng, Y., Hu, H., and Ding, J. (2006) *J. Mol. Biol.* **364,** 1021–1033
64. Scarsdale, J. N., Peculis, B. A., and Wright, H. T. (2006) *Structure* **14,** 331–343
65. Wakamatsu, T., Nakagawa, N., Kuramitsu, S., and Masui, R. (2008) *J. Bacteriol.* **190,** 1108–1117
66. Gabelli, S. B., Bianchet, M. A., Ohnishi, Y., Ichikawa, Y., Bessman, M. J., and Amzel, L. M. (2002) *Biochemistry* **41,** 9279–9285
67. Zha, M., Guo, Q., Zhang, Y., Yu, B., Ou, Y., Zhong, C., and Ding, J. (2008) *J. Mol. Biol.* **379,** 568–578
68. Frick, D. N., Weber, D. J., Gillespie, J. R., Bessman, M. J., and Mildvan, A. S. (1994) *J. Biol. Chem.* **269,** 1794–1803
69. Shimokawa, H., Fujii, Y., Furuichi, M., Sekiguchi, M., and Nakabeppu, Y. (2000) *Nucleic Acids Res.* **28,** 3240–3249
70. Harris, T. K., Wu, G., Massiah, M. A., and Mildvan, A. S. (2000) *Biochemistry* **39,** 1655–1674
71. Mildvan, A. S., Xia, Z., Azurmendi, H. F., Saraswat, V., Legler, P. M., Massiah, M. A., Gabelli, S. B., Bianchet, M. A., Kang, L. W., and Amzel, L. M. (2005) *Arch. Biochem. Biophys.* **433,** 129–143
72. Thompson, J. D., Higgins, D. G., and Gibson, T. J. (1994) *Nucleic Acids Res.* **22,** 4673–4680

HUMAN MUTATION Mutation in Brief 31: E1861-E1874 (2010) Online

MUTATION IN BRIEF

HUMAN MUTATION

Adenine DNA Glycosylase Activity of 14 Human MutY Homolog (MUTYH) Variant Proteins Found in Patients with Colorectal Polyposis and Cancer

OFFICIAL JOURNAL
HGVS
HUMAN GENOME VARIATION SOCIETY
www.hgvs.org

Masanori Goto[1], Kazuya Shinmura[1*], Yusaku Nakabeppu[2], Hong Tao[1], Hidetaka Yamada[1], Toshihiro Tsuneyoshi[3], and Haruhiko Sugimura[1*]

[1]First Department of Pathology, Hamamatsu University School of Medicine, Japan [2]Division of Neurofunctional Genomics, Department of Immunobiology and Neuroscience, Medical Institute of Bioregulation, Kyushu University, Japan [3]Department of Materials and Life Science, Shizuoka Institute of Science and Technology, Japan

*Correspondence to Haruhiko Sugimura, Professor, First Department of Pathology, Hamamatsu University School of Medicine, 1-20-1 Handayama, Higashi Ward, Hamamatsu, Shizuoka 431-3192, Japan. E-mail: hsugimur@hama-med.ac.jp or Kazuya Shinmura, Associate Professor, First Department of Pathology, Hamamatsu University School of Medicine, Hamamatsu, Shizuoka 431-3192, Japan. E-mail: kzshinmu@hama-med.ac.jp

Communicated by Riccardo Fodde

ABSTRACT: Biallelic inactivating germline mutations in the base excision repair *MUTYH (MYH)* gene have been shown to predispose to MUTYH-associated polyposis (MAP), which is characterized by multiple colorectal adenomas and carcinomas. In this study, we successfully prepared highly homogeneous human MUTYH type 2 recombinant proteins and compared the DNA glycosylase activity of the wild-type protein and fourteen variant-type proteins on adenine mispaired with 8-hydroxyguanine, an oxidized form of guanine. The adenine DNA glycosylase activity of the p.I195V protein, p.G368D protein, p.M255V protein, and p.Y151C protein was 66.9%, 15.2%, 10.7%, and 4.5%, respectively, of that of the wild-type protein, and the glycosylase activity of the p.R154H, p.L360P, p.P377L, p.452delE, p.R69X, and p.Q310X proteins as well as of the p.D208N negative control form was extremely severely impaired. The glycosylase activity of the p.V47E, p.R281C, p.A345V, and p.S487F proteins, on the other hand, was almost the same as that of the wild-type protein. These results should be of great value in accurately diagnosing MAP and in fully understanding the mechanism by which MUTYH repairs DNA in which adenine is mispaired with 8-hydroxyguanine. ©2010 Wiley-Liss, Inc.

KEY WORDS: base excision repair, 8-hydroxyguanine, MUTYH, MUTYH-associated polyposis, MAP, DNA glycosylase, colorectal cancer

INTRODUCTION

8-Hydroxyguanine (8-OHG) is an oxidized form of guanine (Kasai and Nishimura, 1991), and because 8-OHG can pair with adenine as well as cytosine, formation of 8-OHG in DNA causes a G:C to T:A transversion mutation (Shibutani et al., 1991). MUTYH protein (MIM# 604933), also known as MYH protein, is a DNA glycosylase that

Received 15 March 2010; accepted revised manuscript 1 September 2010.

DOI: 10.1002/humu.21363

catalyzes the removal of adenine mispaired with 8-OHG in double-stranded DNA (Slupska et al., 1999; Shinmura et al., 2000; Tao et al., 2008). Two major MUTYH proteins, i.e., type 1 and type 2, are expressed in human cells as a result of the presence of multiple transcription initiation sites and alternative splicing of mRNA transcripts (Takao et al., 1999; Ohtsubo et al., 2000). Type 1 is composed of 535 amino acids, and because it contains a mitochondrial targeting signal (MTS) in its N-terminal, it is localized in the mitochondria. Type 2 is composed of only 521 amino acid, because it lacks the N-terminal 14 amino acids of type 1, which contain the MTS, and as a result type 2 is localized in the nucleus (Takao et al., 1999; Ohtsubo et al., 2000). The excisional repair activity of the type 2 protein is greater than that of the type 1 protein under certain conditions (Shinmura et al., 2000).

Biallelic inactivating germline mutations in the *MUTYH* gene predispose to MUTYH-associated polyposis (MAP; MIM# 608456), an autosomal recessive disorder characterized by multiple colorectal adenomas and carcinomas (Al-Tassan et al., 2002; Jones et al., 2002; Sampson et al., 2003; Sieber et al., 2003). Since the diagnosis of MAP depends on the level of repair activity of the MUTYH variants encoded in the two *MUTYH* alleles of the patient and the presence of the clinical phenotype characteristic of MAP, even when *MUTYH* gene variations are present in a patient, information on the level of repair activity of the MUTYH variants is indispensable to making the diagnosis of MAP. However, even though more than 80 MUTYH variants have been described in the *MUTYH* gene in colorectal polyposis and colorectal cancer patients (reviewed in Cheadle and Sampson, 2007; Vogt et al., 2009), the effect of only a small number of variations on human MUTYH protein activity has been investigated (Wooden et al., 2004; Bai et al., 2005; Bai et al., 2007; Ali et al., 2008; Kundu et al., 2009; Forsbring et al., 2009; Molatore et al., 2010). One of the reasons for not investigating the effect of more variations is that human MUTYH recombinant proteins cannot be efficiently overexpressed and purified in *Escherichia coli (E. coli)* and baculovirus cultures or in a cell-free system. Thus, even in previous investigations of variant MUTYH proteins, the purified protein fraction also contained multiple other proteins, judging from the photographs of the SDS-PAGE gels. The authors of one paper (Bai et al., 2005) estimated that the purity of the GST-MUTYH fusion proteins used in the analysis was approximately 15%. Too much amount of contamination by other proteins can interfere with accurate determination of the repair activity of variant MUTYH proteins. Thus, improvement of the production and purification system is needed to enable accurate evaluation of the repair activity of variant MUTYH proteins. Moreover, since somatic *APC* (MIM# 611731) mutations occur in the nuclear DNA of a high proportion of MAP tumors (Al-Tassan et al., 2002), it is preferable to evaluate the repair activity of the type 2 protein localized in the nucleus, not the type 1 mitochondrial protein. However, except for the study by Molatole et al. (2010), the repair activity of variants of the type 1 mitochondrial MUTYH form, not the type 2 nuclear form, has been studied in previous studies. Therefore, in the present study we established an experimental system for the purification of MUTYH type 2 recombinant proteins and evaluated 14 type 2 variants, i.e., p.V47E, p.Y151C, p.R154H, p.I195V, p.M255V, p.R281C, p.A345V, p.L360P, p.G368D, p.P377L, p.452delE, p.S487F, p.R69X, and p.Q310X, which correspond to type 1 proteins p.V61E, p.Y165C, p.R168H, p.I201V, p.M269V, p.R295C, p.A359V, p.L374P, p.G382D, p.P391L, p.466delE, p.S501F, p.R83X, and p.Q324X, respectively. All of the above are MUTYH variants that have been identified in patients with colorectal polyposis and/or with colorectal cancer (Halford et al., 2003; Sieber et al., 2003; Aceto et al., 2005; Aretz et al., 2006; Kanter-Smoler et al., 2006; Lejeune et al., 2006; Peterlongo et al., 2006; Russell et al., 2006; Yanaru-Fujisawa et al., 2008). This study assessed the adenine excisional activity of a larger number of MUTYH variants than in previous studies, and the repair activity of the type 2 protein of 11 of the 14 MUTYH variants (p.V47E, p.R154H, p.I195V, p.M255V, p.R281C, p.A345V, p.L360P, p.P377L, p.S487F, p.R69X, and p.Q310X) was examined for the first in this study.

MATERIALS AND METHODS

Plasmid construction

The human MUTYH type 2 cDNA sequence was inserted into a pET25b(+) expression vector (Novagen, Darmstadt, Germany). The expression vector for 13 missense-type variants was generated by site-directed mutagenesis with a QuikChange Site-directed Mutagenesis kit (Stratagene, La Jolla, CA). The expression vector for p.R69X and p.Q310X types were constructed by inserting MUTYH cDNA sequence (nucleotides 1-204 and 1-927, respectively) into the pET25b(+) expression vector. All vectors were confirmed by DNA sequencing with a BigDye Terminator Cycle Sequencing Reaction Kit (Applied Biosystems, Tokyo, Japan) and an ABI 3100 Genetic Analyzer (Applied Biosystems).

Preparation of the recombinant MUTYH proteins

E. coli BL21-CodonPlus (DE3)-RP competent cells (Stratagene) were transformed with the MUTYH-pET25b vector and cultured at 37°C until an A_{600} of 0.6. After incubation with 0.1 mM IPTG at 15°C for 12 h, MUTYH-His_6 protein was purified with TALON metal affinity resins (Clontech, Palo Alto, CA) and a TALON 2-ml disposable gravity column (Clontech). The protein was then dialyzed against buffer containing 10 mM sodium phosphate (pH 7.6), 50 mM NaCl, 0.5 mM DTT, 0.1 mM EDTA, 0.5 mM PMSF, 2 μg/ml pepstatin, 2 μg/ml leupeptin, 50 μM chymostatin, and 10% glycerol. The quality and concentration of MUTYH proteins were determined by using an Agilent 2100 Bioanalyzer (Agilent Technologies, Palo Alto, CA) and Image J software (National Institutes of Health, Bethesda, MD).

Western blot analysis

Purified recombinant protein was mixed with an equal volume of 2x SDS sample buffer and boiled. A 2 μg protein was subjected to SDS-polyacrylamide gel electrophoresis (PAGE) and electrophoretically transferred to a polyvinylidene difluoride membrane (GE Healthcare Bio-Science Corp., Piscataway, NJ). The membrane was blocked with non-fat milk and incubated with an anti-MUTYH polyclonal antibody (Ohtsubo et al., 2000). After washing, the membrane was incubated with an anti-rabbit HRP-conjugated secondary antibody (GE Healthcare Bio-Science Corp.). The membrane was then washed, and immunoreactivity was visualized with an ECL Plus chemiluminescence system (GE Healthcare Bio-Science Corp.).

DNA cleavage activity assay

30-mer oligonucleotides containing and not containing a single 8-OHG (5'-CTG GTG GCC TGA C[8-OHG or T]C ATT CCC CAA CTA GTG-3') were chemically synthesized and purified by PAGE (Japan Bio Services, Saitama, Japan). Complementary oligonucleotides containing an adenine opposite the 8-OHG or T were ^{32}P-labeled at the 5' terminus with a MEGALABEL kit (Takara, Osaka, Japan) and a [γ-^{32}P]ATP (PerkinElmer, Tokyo, Japan), and then annealed to oligonucleotides containing a single 8-OHG or T. The reaction mixture containing 20 mM sodium phosphate (pH 7.6), 100 mM NaCl, 0.5 mM DTT, 0.5 mM EDTA, 5 μM $ZnCl_2$, 1.5% glycerol, 2.5 nM labeled oligonucleotide, 50 μg/ml BSA, and purified MUTYH protein was incubated at 37°C, and the mixture was treated with 0.1 M NaOH at 95°C for 4 min. After adding denaturing formamide dye to the mixture, it was heated at 95°C for 3 min, and subjected to 20% PAGE. A ^{32}P-labeled marker oligonucleotide was used as a size marker for the cleavage products. The radioactivity of intact and cleaved oligonucleotides was quantified by using an FLA-3000 fluoroimage analyzer (Fuji Film, Tokyo, Japan) and ImageGauge software (Fuji Film) (Goto et al., 2009).

Active site titration and evaluation of the rate constant k_f

The active site titration and evaluation of the rate constant were performed as described previously (Fersht, 1985; Kundu et al., 2009). A 100 ng amount of total proteins was incubated at 37°C for 0 - 30 min with 5 nM 8-OHG containing substrate and the cleavage products were monitored. To determine the amplitude of the burst (A_0), which is proportional to the active protein fraction concentration, the data were fitted to equation (1):

$$[P]_t = A_0[1-\exp(-k_b t)] + k_l t \qquad (1)$$

where $[P]_t$ is the cleavage product concentration at time t and k_b and k_l are the rate constants of the burst phase and the linear phase, respectively.

Rate constant, k_f, was evaluated under single-turnover conditions. A 10 nM concentration of active MUTYH enzymes was incubated at 37°C for 0 - 15 min with 2.5 nM 8-OHG containing substrate and the cleavage products were monitored. To estimate the k_f, the data were fitted to equation (2):

$$[P]_t = A_0[1-\exp(-k_f t)] \qquad (2)$$

Mutation nomenclature and reference sequence

Mutation nomenclature is according to den Dunnen and Antonarakis (2000) and den Dunnen and Paalman (2003). The reference sequence for the *MUTYH* gene encoding type 2 protein is accession number NM_001048174.1. The nucleotide numbering system uses the A of the ATG translation initiation start site as nucleotide +1.

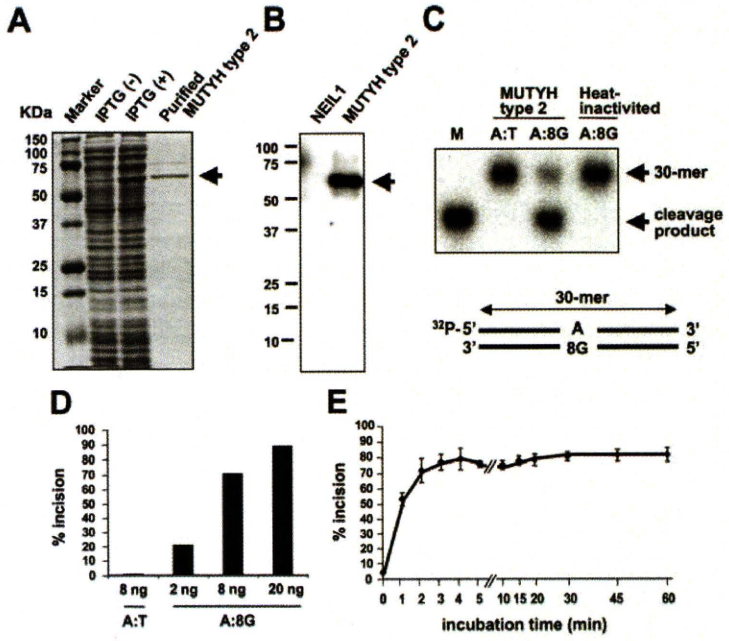

Figure 1. Measurement of the adenine DNA glycosylase activity of wild-type MUTYH type 2 protein. (**A**) Purification of wild-type MUTYH type 2 protein resolved by SDS-polyacrylamide gel electrophoresis (PAGE) and stained with Coomassie Brilliant Blue. Lysates of *E. coli* culture without or with IPTG induction and purified MUTYH type 2 protein are shown. The arrow points to the MUTYH-His_6 protein band. (**B**) Western blot of purified wild-type MUTYH type 2 protein tagged with His_6. MUTYH-His_6 protein is indicated by the arrow. Purified recombinant NEIL1 (MIM# 608844)-His_6 protein, which was prepared by using pET25b(+) vector (Novagen) and *E. coli* BL21-CodonPlus (DE3)-RP cells (Stratagene) previously (Shinmura et al., 2004), was included as a negative control. (**C**) The DNA glycosylase activity of MUTYH type 2 protein on double-stranded DNA containing an A:8-hydroxyguanine (8-OHG). The MUTYH type 2 protein and a ^{32}P-labeled double-stranded oligonucleotides containing or not containing a single 8-OHG mispair were incubated and subjected to 20% PAGE. The intact 30-mer oligonucleotides and cleavage products are indicated by the arrows. Heat-inactivation of the MUTYH protein was accomplished by heating the protein at 100°C for 5 min. 8G means 8-hydroxyguanine. (**D**) Protein concentration dependency of cleavage of DNA containing an A:8-OHG by MUTYH type 2 protein. The MUTYH protein (2, 8, and 20 ng) was incubated at 37°C for 15 min with a 30-mer oligonucleotide containing an A:8-OHG or A:T (50 fmole). The amount of cleavage products as a proportion of total oligonucleotides was calculated as % incision. (**E**) Time-course assay of cleavage of DNA containing an A:8-OHG by MUTYH type 2 protein. The 8 ng amount of MUTYH type 2 protein was incubated at 37°C for 0 - 60 min with double-stranded oligonucleotide containing an A:8-OHG (50 fmole). The % incision valves are means ± standard errors of data from three independent experiments.

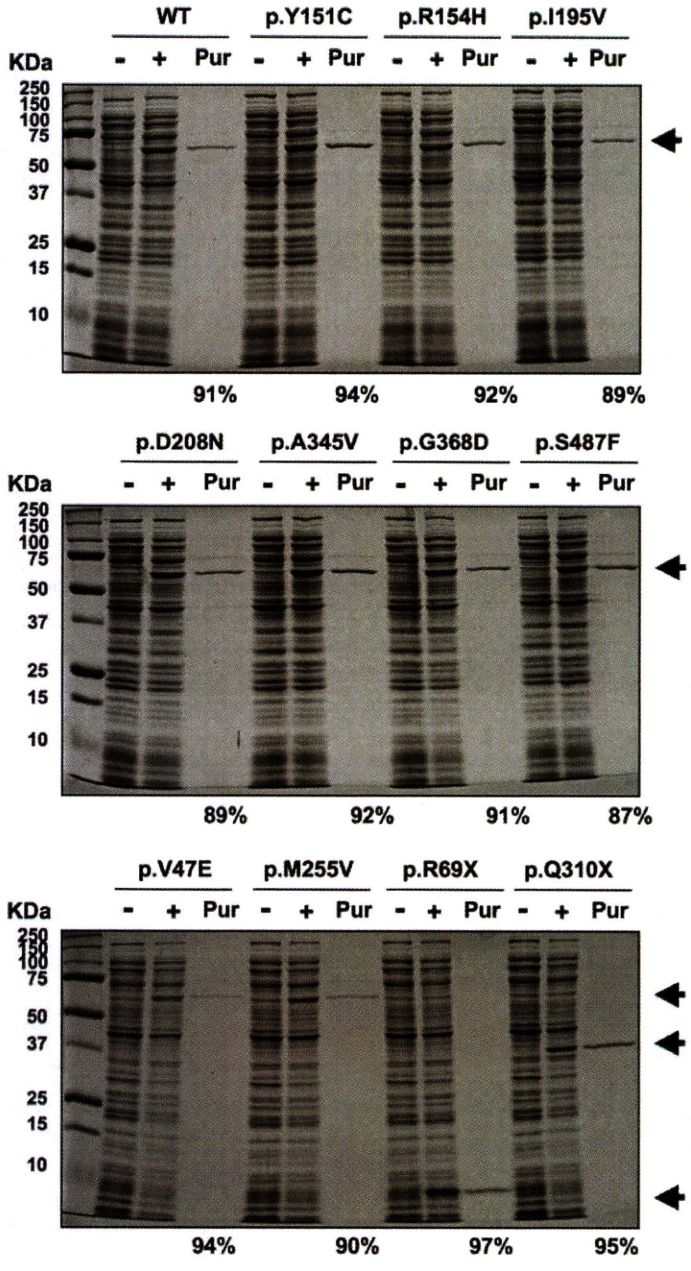

Figure 2. Purification of variant-type MUTYH type 2 recombinant proteins. Each protein was overexpressed and purified under conditions essentially the same as used for the wild-type (WT) protein. Representative results of expression and purification of MUTYH proteins resolved by SDS-PAGE and stained with Coomassie Brilliant Blue are shown. '–' and '+' mean absence and presence, respectively, of IPTG induction, and 'Pur' means purified MUTYH type 2 proteins. The arrow points to the MUTYH-His_6 protein band. The purification level is indicated below the SDS-PAGE panels.

RESULTS

To overcome the difficulty of preparing highly purified recombinant MUTYH proteins, in this study, we used a pET25b(+) expression vector and BL21-CodonPlus (DE3)-RP *E. coli* host cells for induction of MUTYH expression and a TALON metal affinity resin and gravity column for purification of the MUTYH proteins. Wild-type human MUTYH type 2 protein tagged with His_6 at its C-terminus was successfully overexpressed in *E. coli* and purified to approximately 90% homogeneity (Figure 1A). The specificity of the purified MUTYH protein was confirmed by Western blotting with anti-MUTYH polyclonal antibody (Figure 1B). Their molecular size of approximately 61 kDa was determined by SDS-PAGE / Coomassie Brilliant Blue (CBB) staining and Western blotting, and it corresponded to their size calculated from the cDNA sequence. The DNA glycosylase activity of the wild-type MUTYH protein was tested by determining its capacity to cleave a double-stranded oligonucleotide containing an adenine mispaired with 8-OHG. The cleavage products were analyzed on a denaturing polyacrylamide gel, and their mobility was compared with that of a marker oligonucleotide. No clear cleavage products were detected when oligonucleotide containing an unmodified A:T base pair was exposed to the MUTYH protein, but cleavage products having the same mobility as the marker oligonucleotide were detected when MUTYH proteins were allowed to react with oligonucleotide containing an A:8-OHG base pair (Figure 1C). No cleavage was detected when allowed to react after heat-inactivation of the MUTYH protein (Figure 1C). The amount of cleavage products was calculated as percent of total oligonucleotides and expressed as % incision, and the % incision of protein substrate containing an A:8-OHG mispair increased in a protein-concentration–dependent manner (Figure 1D). The time-course assay of the cleavage activity of MUTYH protein on substrate containing an A:8-OHG mispair indicated that the amount of cleavage products peaked within 5 min and was almost constant from 5 min to 60 min (Figure 1E). The results showed that highly purified wild-type MUTYH type 2 protein had been obtained with our expression and purification system, and the adenine DNA glycosylase activity of the protein on an A:8-OHG mispair was satisfactorily detected by our assay. We therefore decided to apply our experimental systems to assessment of the adenine DNA glycosylase activity of various MUTYH variant proteins.

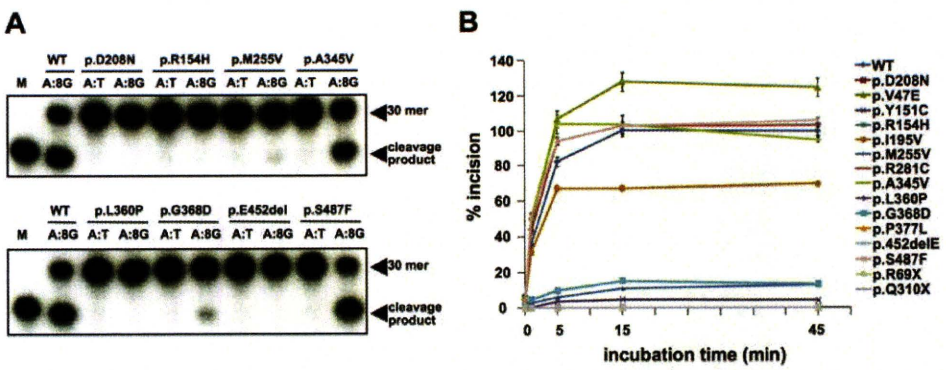

Figure 3. Measurement of the adenine DNA glycosylase activity of variant MUTYH type 2 proteins. **(A)** Representative results of DNA cleavage assays of MUTYH variant proteins are shown. MUTYH proteins (130 fmole) were allowed to act on double-stranded oligonucleotide containing a single A:8-OHG (8G) mispair at 37°C for 15 min. The reaction mixture was analyzed by 20% PAGE. A ^{32}P-labeled marker oligonucleotide was used as a size marker for the cleavage products. The intact 30-mer oligonucleotides and cleavage products are indicated by the arrows. **(B)** Time-course assay of cleavage of DNA containing an A:8-OHG by MUTYH type 2 protein. MUTYH type 2 proteins (130 fmole) were incubated at 37°C for 0 - 45 min with double-stranded oligonucleotide containing an A:8-OHG (50 fmole). The amount of cleavage products as a proportion of total oligonucleotides was calculated as % incision, and the % incision of each variant-type MUTYH protein is shown relative to that of wild-type (WT) MUTYH protein, which has been set equal to 100. The % incision valves are means ± standard errors of data obtained from three independent experiments in which three independently prepared MUTYH proteins were used.

Table 1. DNA glycosylase activity of 14 variants of MUTYH type 2 protein on DNA containing adenine mispaired with 8-hydroxyguanine

MUTYH type 2 protein	Type of mutation[a]	Purified protein yield (ng) per 10 ml culture[b]	Relative % incision[c]
WT		4365, 3562, 3454	100
p.D208N	negative control	2073, 1826, 1808	extremely severely defective
p.V47E	c.140T>A, missense	1018, 1893, 1916	128.1±5.20
p.Y151C	c.452A>G, missense	5485, 4779, 2835	4.5±0.21
p.R154H	c.461G>A, missense	894, 1501, 2109	extremely severely defective
p.I195V	c.583A>G, missense	1733, 1102, 671	66.9±0.35
p.M255V	c.763A>G, missense	2446, 1726, 2488	10.7±0.47
p.R281C	c.841C>T, missense	912, 934, 447	103.0±1.39
p.A345V	c.1034C>T, missense	2564, 2435, 3864	103.5±5.43
p.L360P	c.1079T>C, missense	152, 303, 120	extremely severely defective
p.G368D	c.1103G>A, missense	2486, 1246, 2270	15.2±0.71
p.P377L	c.1130C>T, missense	885, 626, 430	extremely severely defective
p.452delE	c.1353_1355delGGA, inframe deletion	822, 614, 364	extremely severely defective
p.S487F	c.1460C>T, missense	1099, 984, 706	102.8±2.31
p.R69X	c.205C>T, nonsense	6289, 5245, 6289	extremely severely defective
p.Q310X	c.928C>T, nonsense	918, 5726, 2771	extremely severely defective

[a]The reference sequence for the *MUTYH* gene encoding type 2 protein is accession number NM_001048174.1.

[b]Amount of MUTYH proteins purified from 10 ml of *E. coli* culture expressing MUTYH type 2 protein. Each protein was purified three times and has been listed in this table.

[c]The DNA cleavage activity of MUTYH protein was measured under conditions of 37°C for 15 min. The amount of cleavage products as a proportion of total oligonucleotides was calculated as % incision, and the % incision of each variant-type MUTYH protein is shown relative to that of wild-type (WT) MUTYH protein, which has been set equal to 100. Values are means ± standard errors of data obtained from three independent experiments in which three independently prepared MUTYH proteins were used.

Fourteen MUTYH variants that had previously been identified in patients with colorectal polyposis and/or colorectal cancer were selected, and their expression vectors were prepared by site-directed mutagenesis. Since the Asp222 in MUTYH type 1 is the active site, and the p.D222N mutant is known not to have DNA glycosylase activity (Wooden et al., 2004), we prepared a type 2-p.D208N construct corresponding to type 1-p.D222N as a negative control. A total of 15 MUTYH type 2 proteins were successfully expressed and purified to a high level of homogeneity (Figure 2). Their molecular sizes determined by SDS-PAGE / CBB staining corresponded with their sizes calculated from their cDNA sequences. Each MUTYH variant protein was almost always reproducibly obtained in the three independent protein preparation (Table 1). Next, we compared the DNA glycosylase activity of each variant protein on oligonucleotide containing an A:8-OHG mispair with that of the wild-type MUTYH type 2 protein (Figure 3 and Table 1). As expected, no clear cleavage products were detected when any of the variant proteins were allowed to act on oligonucleotide containing an unmodified A:T base pair (Figure 3). The adenine DNA glycosylase activity of the MUTYH variant proteins on oligonucleotide containing an A:8-OHG mispair varied (Figure 3 and Table 1). The adenine DNA glycosylase activity of the p.V47E, p.R281C, p.A345V, and p.S487F proteins on the A:8-OHG substrate under conditions of 37°C for 15 min were similar to that of the wild-type protein or only slightly different (102.8% - 128.1%, with activity of the wild-type protein set equal to 100%), whereas p.I195V protein exhibited slightly lower glycosylase activity (66.9%). The p.Y151C protein, p.M255V protein and p.G368D protein exhibited only 4.5%, 10.7%, and 15.2%, respectively, of the glycosylase activity of the wild-type protein, and the adenine DNA glycosylase activity of the p.R154H, p.L360P, p.P377L, p.452delE, p.R69X, and p.Q310X proteins as well as of the p.D208N negative control protein was almost at the background

level. We also attempted to determine whether the recombinant type 1 variant proteins had a level of repair activity that was similar to that of the corresponding type 2 proteins. We randomly chose type 1-p.R168H and type 1-p.S501F, which correspond to type 2-p.R154H and type 2-p.S487F, respectively, and found that the activity level of the type 1 and type 2 proteins of at least these two MUTYH variants in comparison with the wild-type protein is similar (Supp. Figure S1A-E). We also estimated the rate constant k_f of some type 2 proteins on the A:8-OHG substrate after correction for the active enzyme fraction as described previously (Fersht, 1985; Kundu et al., 2009). The rate constant for adenine excision by wild-type protein was 0.524, and similar to the constant for p.R281C (k_f = 0.489) (Table 2). However, the k_f value of p.M255V was 0.024 and more than 20-fold lower than that of the wild-type protein, indicating that the glycosylase activity of p.M255V was severely reduced. The above findings indicate that the adenine DNA glycosylase activity of nine of the 14 MUTYH type 2 variant proteins tested is severely impaired.

Table 2. Active yield and rate constant k_f evaluated for MUTYH type 2 protein on DNA containing adenine mispaired with 8-hydroxyguanine

MUTYH type 2 protein	Active protein yield (μg) per 1L culture[a]	k_f (min^{-1})[b]
WT	2706, 1248, 2045	0.524±0.034
p.M255V	58, 72, 75	0.024±0.004
p.R281C	944, 1128, 751	0.489±0.044

[a]Values were obtained by incubating 100 ng of total proteins with 5 nM of substrate. Results obtained with three separate protein preparations are shown.

[b]Values were obtained by incubating 10 nM of active MUTYH enzyme and 2.5 nM of substrate. Values are means ± standard errors of data obtained from three independent experiments using independently prepared proteins.

DISCUSSION

The cumulative results of recent screenings of colorectal polyposis patients for *MUTYH* mutations have revealed many *MUTYH* gene variants (reviewed in Cheadle and Sampson, 2007; Vogt et al., 2009), but the repair activity of the type 2 protein of most of the variants has never been tested. In this study we improved the method of expressing and purifying the recombinant MUTYH type 2 proteins and assessed the adenine DNA glycosylase activity of various type 2 proteins. The results revealed that the p.V47E, p.R281C, p.A345V, and p.S487F proteins largely retain adenine removing activity, but that the adenine removing activity of the p.I195V protein is mildly impaired and the activity of the p.Y151C, p.R154H, p.M255V, p.L360P, p.G368D, p.P377L, p.452delE, p.R69X, and p.Q310X proteins is severely impaired. This information should be of great help in accurately diagnosing MAP and managing MAP patients.

The adenine DNA glycosylase activity of the type 1 or type 2 MUTYH variants p.Y151C, p.G368D, p.P377L, p.452delE, and p.S487F has been assessed previously (Wooden et al., 2004; Ali et al., 2008; Kundu et al., 2009; Forsbring et al., 2009; Molatore et al., 2010). The results showed that the repair activity of p.Y151C, p.G368D, p.P377L, and p.452delE was impaired while that of p.S487F was retained, findings that were consistent with our own, and the consistency confirms the reliability of the results of our study. Interestingly, a slight difference (approximately 5% vs. approximately 15%) in repair activity was observed between p.Y151C and p.G368D in our study, and the same difference was reported in several previous papers. Nielsen et al. (2009) recently reported finding that MAP patients homozygous for a p.G368D allele have a milder clinical phenotype than MAP patients homozygous for a p.Y151C allele. The difference in adenine removing activity between the p.Y151C protein and p.G368D protein may be related to the difference in clinical phenotype.

Retention of DNA glycosylase activity by the human MUTYH proteins p.V47E, p.R281C, and p.A345V as well as mild impairment of the activity of p.I195V and severe impairment of the activity of p.R154H, p.M255V, p.L360P, p.R69X, and p.Q310X were documented for the first time in this study. Although no analyses of crystal

structure of the MUTYH has been reported, based on the cumulative results of previous studies of the biochemistry of MUTYH (reviewed in Cheadle and Sampson, 2007; Ali et al., 2008), p.R154, p.M255, and p.L360 are located in regions suspected of being important to catalytic activity or substrate recognition. Moreover, the p.R154, p.M255, and p.L360 in MUTYH protein are conserved among *E. coli*, *Mus musculus*, *Rattus norvegicus*, *Pan troglodytes*, *Canis familiaris*, and *Homo sapiens*. Substitution of any of these amino acids appears to result in a functional abnormality, resulting in severe reduction of adenine DNA glycosylase activity on DNA containing an A:8-OHG mispair. The loss of large parts of the MUTYH protein in the frameshift-type variant proteins p.R69X and p.Q310X may be responsible for the severe impairment of their adenine removing activity. An amino acid substitution in p.V47E, p.R281C, p.A345V, and p.S487F did not greatly affect their adenine DNA glycosylase activity. These results are consistent with the prediction of a possible impact of an amino acid substitution on the structure and function of MUTYH type 2 protein by the PolyPhen-2 program (http://genetics.bwh.harvard.edu/pph2/index.shtml) (Adzhubei et al., 2010). Since p.V47E, p.R281C, p.A345V, and p.S487F are not located in the region suspected of being important to catalytic activity or in a well-conserved position of the substrate recognition region, the amino acid localization may be one of the reasons for the retention of enzymatic activity. In the future, a crystal structure of the MUTYH protein alone and covalently complexed with DNA, in conjunction with the present findings on MUTYH variants, should contribute to establishing further correlations between the structure and repair function of the MUTYH protein.

Highly homogeneous MUTYH type 2 recombinant protein was prepared by using the method described in this study. As far as we have been able to determine in a review of the literature, the level of purification of the proteins in our study was higher than level of purification estimated from the SDS-PAGE images of MUTYH type 1 or type 2 proteins in previous papers and purification levels described in the other papers. Use of *E. coli* BL21-CodonPlus (DE3)-RP cells, which contain extra copies of the genes that encode the tRNAs of rare *E. coli* codons, is thought to be responsible for the increase in level of MUTYH protein expression, because the *MUTYH* gene contains many rare codons. The expression conditions (temperature and IPTG concentration), combination of expression vector and competent cells, and metal-affinity purification conditions are also thought to possibly have contributed to the improvement in the level of purification in this study. Since genetic screening of colorectal polyposis patients for *MUTYH* mutations will continue to be performed worldwide, the same as genetic screening for *APC* mutations (reviewed in Lynch et al., 2008), our method of expression and purification of human MUTYH protein should be useful for assessing MUTYH variants newly identified by genetic screening as well as MUTYH variants that have not been examined.

As shown in Supp. Figure S1E, the activity level of the type 1 and type 2 proteins of two MUTYH variants in comparison with the wild-type protein was similar. Although comparisons were not made for the other variants, it may not always be necessarily to study the type 2 form when analyzing MUTYH protein. However, since type 2, and not type 1, is a nuclear form (Takao et al., 1999; Ohtsubo et al., 2000), and somatic *APC* mutations occur in the nuclear DNA of MAP tumors (Al-Tassan et al., 2002), we think that evaluation of type 2 variants is likely to be more preferable when we investigate the possible pathogenic role of MUTYH in MAP. Assessment of the glycosylase activity level of the wild-type type 1 and type 2 proteins showed that the activity of type 2 was greater than that of type 1 (Figure 1 and Supp. Figure S1), a finding that is consistent with a previous report (Shinmura et al., 2000). The reason for the difference in the catalysis of adenine excision between the type 1 and type 2 proteins is unclear. One point that requires caution is that there is evidence that the type 1 protein is processed during mitochondrial transport in cells and the mature form of the protein never been identified, and thus the repair activity of the full-length type 1 may not necessarily reflect the activity *in vivo*. With regard to the method of evaluating MUTYH variant proteins, since MUTYH possesses suppressive activity against G:C to T:A mutations caused by 8-OHG (Yamane et al., 2003) and biallelic *MUTYH* inactivation leads to somatic *APC* mutation in MAP tumors (Al-Tassan et al., 2002), analysis of the mutation rate of the *APC* gene in MUTYH variant-expressing cells may be an alternative way of evaluating the level of repair activity of a MUTYH variant. A combination of mutation rate analysis and DNA glycosylase analysis would provide more definitive proof of the pathogenicity of a MUTYH variant.

ACKNOWLEDGMENTS

Contract grant sponsor: The Ministry of Health, Labour and Welfare for the Comprehensive 10-Year Strategy for Cancer Control (19-19) and the Third Term Comprehensive Control Research for Cancer, the Japan Society for the

Promotion of Science for Scientific Research (19790286, 22590356, 22790378), the Ministry of Education, Culture, Sports, Science and Technology for priority area (18014009, 20014007, 221S0001), and the Smoking Research Foundation.

REFERENCES

Aceto G, Cristina Curia M, Veschi S, De Lellis L, Mammarella S, Catalano T, Stuppia L, Palka G, Valanzano R, Tonelli F, Casale V, Stigliano V, Cetta F, Battista P, Mariani-Costantini R, Cama A. 2005. Mutations of APC and MYH in unrelated Italian patients with adenomatous polyposis coli. Hum Mutat 26: 394.

Adzhubei IA, Schmidt S, Peshkin L, Ramensky VE, Gerasimova A, Bork P, Kondrashov AS, Sunyaev SR. 2010. A method and server for predicting damaging missense mutations. Nat Methods 7:248-9.

Al-Tassan N, Chmiel NH, Maynard J, Fleming N, Livingston AL, Williams GT, Hodges AK, Davies DR, David SS, Sampson JR, Cheadle JP. 2002. Inherited variants of MYH associated with somatic G:C-->T:A mutations in colorectal tumors. Nat Genet 30: 227-32.

Ali M, Kim H, Cleary S, Cupples C, Gallinger S, Bristow R. 2008. Characterization of mutant MUTYH proteins associated with familial colorectal cancer. Gastroenterology 135: 499-507.

Aretz S, Uhlhaas S, Goergens H, Siberg K, Vogel M, Pagenstecher C, Mangold E, Caspari R, Propping P, Friedl W. 2006. MUTYH-associated polyposis: 70 of 71 patients with biallelic mutations present with an attenuated or atypical phenotype. Int J Cancer 119: 807-14.

Bai H, Jones S, Guan X, Wilson TM, Sampson JR, Cheadle JP, Lu AL. 2005. Functional characterization of two human MutY homolog (hMYH) missense mutations (R227W and V232F) that lie within the putative hMSH6 binding domain and are associated with hMYH polyposis. Nucleic Acids Res 33: 597-604.

Bai H, Grist S, Gardner J, Suthers G, Wilson TM, Lu AL. 2007. Functional characterization of human MutY homolog (hMYH) missense mutation (R231L) that is linked with hMYH-associated polyposis. Cancer Lett 250: 74-81.

Cheadle JP, Sampson JR. 2007. MUTYH-associated polyposis--from defect in base excision repair to clinical genetic testing. DNA Repair (Amst) 6: 274-9.

den Dunnen JT, Antonarakis SE. 2000. Mutation nomenclature extensions and suggestions to describe complex mutations: a discussion. Hum Mutat 15:7-12.

den Dunnen JT, Paalman MH. 2003. Standardizing mutation nomenclature: why bother? Hum Mutat 22(3):181-182.

Fersht A. 1985. Measurement and magnitude of enzymatic rate constants. In: Enzyme Structure and Mechanism (2nd edn.). Freeman WH, New York, p 121– 154.

Forsbring M, Vik ES, Dalhus B, Karlsen TH, Bergquist A, Schrumpf E, Bjørås M, Boberg KM, Alseth I. 2009. Catalytically impaired hMYH and NEIL1 mutant proteins identified in patients with primary sclerosing cholangitis and cholangiocarcinoma. Carcinogenesis 30: 1147-54.

Goto M, Shinmura K, Igarashi H, Kobayashi M, Konno H, Yamada H, Iwaizumi M, Kageyama S, Tsuneyoshi T, Tsugane S, Sugimura H. 2009. Altered expression of the human base excision repair gene NTH1 in gastric cancer. Carcinogenesis 30: 1345-52.

Halford SE, Rowan AJ, Lipton L, Sieber OM, Pack K, Thomas HJ, Hodgson SV, Bodmer WF, Tomlinson IP. 2003. Germline mutations but not somatic changes at the MYH locus contribute to the pathogenesis of unselected colorectal cancers. Am J Pathol 162: 1545-8.

Jones S, Emmerson P, Maynard J, Best JM, Jordan S, Williams GT, Sampson JR, Cheadle JP. 2002. Biallelic germline mutations in MYH predispose to multiple colorectal adenoma and somatic G:C-->T:A mutations. Hum Mol Genet 11: 2961-7.

Kanter-Smoler G, Björk J, Fritzell K, Engwall Y, Hallberg B, Karlsson G, Grönberg H, Karlsson P, Wallgren A, Wahlström J, Hultcrantz R, Nordling M. 2006. Novel findings in Swedish patients with MYH-associated polyposis: mutation detection and clinical characterization. Clin Gastroenterol Hepatol 4: 499-506.

Kasai H, Nishimura S. 1991. Formation of 8-hydroxyguanosine in DNA by oxygen radicals and its biological significance. In Sies H. (ed.), Oxidative Stress: Oxidants and Antioxidants. Academic Press, London, UK, p 99-116.

Kundu S, Brinkmeyer MK, Livingston AL, David SS. 2009. Adenine removal activity and bacterial complementation with the human MutY homologue (MUTYH) and Y165C, G382D, P391L and Q324R variants associated with colorectal cancer. DNA Repair (Amst) 8: 1400-10.

Lejeune S, Guillemot F, Triboulet JP, Cattan S, Mouton C; PAFNORD Group, Porchet N, Manouvrier S, Buisine MP. 2006. Low frequency of AXIN2 mutations and high frequency of MUTYH mutations in patients with multiple polyposis. Hum Mutat 27: 1064.

Lynch HT, Lynch JF, Lynch PM, Attard T. 2008. Hereditary colorectal cancer syndromes: molecular genetics, genetic counseling, diagnosis and management. Fam Cancer 7: 27-39.

Molatore S, Russo MT, D'Agostino VG, Barone F, Matsumoto Y, Albertini AM, Minoprio A, Degan P, Mazzei F, Bignami M, Ranzani GN. 2010. MUTYH mutations associated with familial adenomatous polyposis: functional characterization by a mammalian cell-based assay. Hum Mutat 31: 159-66.

Nielsen M, Joerink-van de Beld MC, Jones N, Vogt S, Tops CM, Vasen HF, Sampson JR, Aretz S, Hes FJ. 2009. Analysis of MUTYH genotypes and colorectal phenotypes in patients With MUTYH-associated polyposis. Gastroenterology 136: 471-6.

Ohtsubo T, Nishioka K, Imaiso Y, Iwai S, Shimokawa H, Oda H, Fujiwara T, Nakabeppu Y. 2000. Identification of human MutY homolog (hMYH) as a repair enzyme for 2-hydroxyadenine in DNA and detection of multiple forms of hMYH located in nuclei and mitochondria. Nucleic Acids Res 28: 1355-64.

Peterlongo P, Mitra N, Sanchez de Abajo A, de la Hoya M, Bassi C, Bertario L, Radice P, Glogowski E, Nafa K, Caldes T, Offit K, Ellis NA. 2006. Increased frequency of disease-causing MYH mutations in colon cancer families. Carcinogenesis 27: 2243-9.

Russell AM, Zhang J, Luz J, Hutter P, Chappuis PO, Berthod CR, Maillet P, Mueller H, Heinimann K. 2006. Prevalence of MYH germline mutations in Swiss APC mutation-negative polyposis patients. Int J Cancer 118: 1937-40.

Sampson JR, Dolwani S, Jones S, Eccles D, Ellis A, Evans DG, Frayling I, Jordan S, Maher ER, Mak T, Maynard J, Pigatto F, Shaw J, Cheadle JP. 2003. Autosomal recessive colorectal adenomatous polyposis due to inherited mutations of MYH. Lancet 362: 39-41.

Shibutani S, Takeshita M, Grollman AP. 1991. Insertion of specific bases during DNA synthesis past the oxidation-damaged base 8-oxodG. Nature 349: 431-4.

Shinmura K, Tao H, Goto M, Igarashi H, Taniguchi T, Maekawa M, Takezaki T, Sugimura H. 2004. Inactivating mutations of the human base excision repair gene NEIL1 in gastric cancer. Carcinogenesis 25: 2311-7.

Shinmura K, Yamaguchi S, Saitoh T, Takeuchi-Sasaki M, Kim SR, Nohmi T, Yokota J. 2000. Adenine excisional repair function of MYH protein on the adenine:8-hydroxyguanine base pair in double-stranded DNA. Nucleic Acids Res 28: 4912-8.

Sieber OM, Lipton L, Crabtree M, Heinimann K, Fidalgo P, Phillips RK, Bisgaard ML, Orntoft TF, Aaltonen LA, Hodgson SV, Thomas HJ, Tomlinson IP. 2003. Multiple colorectal adenomas, classic adenomatous polyposis, and germ-line mutations in MYH. N Engl J Med 348: 791-9.

Slupska MM, Luther WM, Chiang JH, Yang H, Miller JH. 1999. Functional expression of hMYH, a human homolog of the *Escherichia coli* MutY protein. J Bacteriol 181: 6210–3.

Takao M, Zhang QM, Yonei S, Yasui A. 1999. Differential subcellular localization of human MutY homolog (hMYH) and the functional activity of adenine:8-oxoguanine DNA glycosylase. Nucleic Acids Res 27: 3638-44.

Tao H, Shinmura K, Suzuki M, Kono S, Mibu R, Tanaka M, Kakeji Y, Maehara Y, Okamura T, Ikejiri K, Futami K, Yasunami Y, Maekawa T, Takenaka K, Ichimiya H, Imaizumi N, Sugimura H. 2008. Association between genetic polymorphisms of the base excision repair gene MUTYH and increased colorectal cancer risk in a Japanese population. Cancer Sci 99: 355-60.

Vogt S, Jones N, Christian D, Engel C, Nielsen M, Kaufmann A, Steinke V, Vasen HF, Propping P, Sampson JR, Hes FJ, Aretz S. 2009. Expanded extracolonic tumor spectrum in MUTYH-associated polyposis. Gastroenterology 137: 1976-85.

Wooden SH, Bassett HM, Wood TG, McCullough AK. 2004. Identification of critical residues required for the mutation avoidance function of human MutY (hMYH) and implications in colorectal cancer. Cancer Lett 205: 89-95.

Yamane A, Shinmura K, Sunaga N, Saitoh T, Yamaguchi S, Shinmura Y, Yoshimura K, Murakami H, Nojima Y, Kohno T, Yokota J. 2003. Suppressive activities of OGG1 and MYH proteins against G:C to T:A mutations caused by 8-hydroxyguanine but not by benzo[a]pyrene diol epoxide in human cells in vivo. Carcinogenesis 24: 1031-7.

Yanaru-Fujisawa R, Matsumoto T, Ushijima Y, Esaki M, Hirahashi M, Gushima M, Yao T, Nakabeppu Y, Iida M. 2008. Genomic and functional analyses of MUTYH in Japanese patients with adenomatous polyposis. Clin Genet 73: 545-53.

SUPPORTING INFORMATION

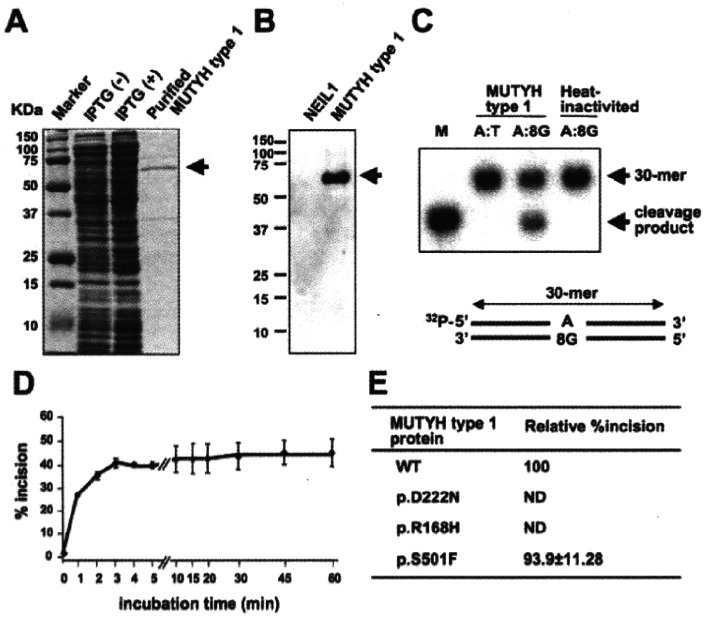

Supp. Figure S1. Measurement of DNA glycosylase activity of MUTYH type 1 protein. (**A**) Purification of wild-type MUTYH type 1 protein resolved by SDS-polyacrylamide gel electrophoresis (PAGE) and stained with Coomassie Brilliant Blue (CBB). The human MUTYH type 1 cDNA sequence was inserted into a pET25b(+) expression vector (Novagen, Darmstadt, Germany). *E. coli* BL21-CodonPlus (DE3)-RP competent cells (Stratagene, La Jolla, CA) were transformed with the MUTYH-pET25b vector and cultured at 37°C until an A_{600} of 0.6. After incubation with 0.1 mM IPTG at 20°C for 12 h, MUTYH-His_6 protein was purified with TALON metal affinity resins (Clontech, Palo Alto, CA) and a TALON 2-ml disposable gravity column (Clontech). The protein was then dialyzed against buffer containing 10 mM sodium phosphate (pH 7.6), 50 mM NaCl, 0.5 mM DTT, 0.1 mM EDTA, 0.5 mM PMSF, 2 μg/ml pepstatin, 2 μg/ml leupeptin, 50 μM chymostatin, and 10% glycerol. Lysates of *E. coli* culture without or with IPTG induction and purified MUTYH type 1 protein are shown. The arrow points to the MUTYH-His_6 protein band. (**B**) Western blot of purified wild-type MUTYH type 1 protein tagged with His_6. Purified recombinant NEIL1-His_6 protein, which was prepared by using pET25b(+) vector (Novagen) and *E. coli* BL21-CodonPlus (DE3)-RP cells (Stratagene) previously (Shinmura et al., 2004), was included as a negative control. Purified recombinant protein was mixed with an equal volume of 2x SDS sample buffer and boiled. A 2 μg protein was subjected to SDS-PAGE and electrophoretically transferred to a polyvinylidene difluoride membrane (GE Healthcare Bio-Science Corp., Piscataway, NJ). The membrane was blocked with non-fat milk and incubated with an anti-MUTYH polyclonal antibody (Ohtsubo et al., 2000). After washing, the membrane was incubated with an anti-rabbit HRP-conjugated secondary antibody (GE Healthcare Bio-Science Corp.). The membrane was then washed, and immunoreactivity was visualized with an ECL Plus chemiluminescence system (GE Healthcare Bio-Science Corp.). MUTYH-His_6 protein is indicated by the arrow. (**C**) The DNA glycosylase activity of wild-type MUTYH type 1 protein on double-stranded DNA containing an A:8-hydroxyguanine (8-OHG). 30-mer oligonucleotides containing and not containing a single 8-OHG (5'-CTG GTG GCC TGA C[8-OHG or T]C ATT CCC CAA CTA GTG-3') were chemically synthesized and purified by PAGE (Japan Bio Services, Saitama, Japan). Complementary oligonucleotides containing an adenine opposite the 8-OHG or T were ^{32}P-labeled at the 5' terminus with a MEGALABEL kit (Takara, Osaka, Japan) and a [γ-^{32}P]ATP (PerkinElmer, Tokyo, Japan), and then annealed to oligonucleotides containing a single 8-OHG or T. The reaction mixture containing 20 mM sodium phosphate (pH 7.6), 100 mM NaCl, 0.5 mM DTT, 0.5 mM EDTA, 5 μM $ZnCl_2$, 1.5% glycerol, 2.5 nM labeled oligonucleotide, 50 μg/ml BSA, and purified MUTYH protein was incubated at 37°C, and the mixture was treated with 0.1 M

NaOH at 95°C for 4 min. After adding denaturing formamide dye to the mixture, it was heated at 95°C for 3 min, and subjected to 20% PAGE. A ^{32}P-labeled marker oligonucleotide was used as a size marker for the cleavage products. The radioactivity of intact and cleaved oligonucleotides was quantified by using an FLA-3000 fluoroimage analyzer (Fuji Film, Tokyo, Japan) and ImageGauge software (Fuji Film) (Goto et al., 2009). The intact 30-mer oligonucleotides and cleavage products are indicated by the arrows. Heat-inactivation of the MUTYH protein was accomplished by heating the protein at 100°C for 5 min. 8G means 8-hydroxyguanine. (**D**) Time-course assay of cleavage of DNA containing an A:8-OHG by wild-type MUTYH type 1 protein. The MUTYH type 1 protein (260 fmole) was incubated at 37°C for 0 - 60 min with double-stranded oligonucleotide containing an A:8-OHG (50 fmole). The amount of cleavage products as a proportion of total oligonucleotides was calculated as % incision. The % incision values are shown as means ± standard errors of data from three independent experiments. (**E**) DNA glycosylase activities of wild-type MUTYH type 1 protein and their variant proteins on an A:8-OHG substrate. DNA cleavage activities of MUTYH type 1 proteins were measured at 37°C for 15 min. The amount of cleavage products as a proportion of total oligonucleotides was calculated as % incision, and the % incision of each variant-type MUTYH protein is shown relative to that of wild-type (WT) MUTYH protein, which has been set equal to 100. Values are means ± standard errors of data from three independent experiments. ND, not detected.

Detection of Lipid Peroxidation-Induced DNA Adducts Caused by 4-Oxo-2(*E*)-nonenal and 4-Oxo-2(*E*)-hexenal in Human Autopsy Tissues

Pei-Hsin Chou,[†,‡] Shinji Kageyama,[§] Shun Matsuda,[†] Keishi Kanemoto,[†] Yoshiaki Sasada,[†] Megumi Oka,[†] Kazuya Shinmura,[§] Hiroki Mori,[§] Kazuaki Kawai,[∥] Hiroshi Kasai,[∥] Haruhiko Sugimura,*[,§] and Tomonari Matsuda*[,†]

Research Center for Environmental Quality Management, Kyoto University, Otsu, Shiga, 520-0811, Japan, Department of Environmental Engineering, National Cheng Kung University, Tainan, 70101, Taiwan, Department of Pathology, Hamamatsu University School of Medicine, Hamamatsu, Shizuoka, 431-3192, Japan, and Department of Environmental Oncology, University of Occupational and Environmental Health, Kitakyushu, Fukuoka, 807-8555, Japan

Received February 8, 2010

DNA adducts are produced both exogenously and endogenously via exposure to various DNA-damaging agents. Two lipid peroxidation (LPO) products, 4-oxo-2(*E*)-nonenal (4-ONE) and 4-oxo-2(*E*)-hexenal (4-OHE), induce substituted etheno-DNA adducts in cells and chemically treated animals, but the adduct levels in humans have never been reported. It is important to investigate the occurrence of 4-ONE- and 4-OHE-derived DNA adducts in humans to further understand their potential impact on human health. In this study, we conducted DNA adductome analysis of several human specimens of pulmonary DNA as well as various LPO-induced DNA adducts in 68 human autopsy tissues, including colon, heart, kidney, liver, lung, pancreas, small intestine, and spleen, by liquid chromatography tandem mass spectrometry. In the adductome analysis, DNA adducts derived from 4-ONE and 4-OHE, namely, heptanone-etheno-2′-deoxycytidine (HεdC), heptanone-etheno-2′-deoxyadenosine (HεdA), and butanone-etheno-2′-deoxycytidine (BεdC), were identified as major adducts in one human pulmonary DNA. Quantitative analysis revealed 4-ONE-derived HεdC, HεdA, and heptanone-etheno-2′-deoxyguanosine (HεdG) to be ubiquitous in various human tissues at median values of 10, 15, and 8.6 adducts per 10^8 bases, respectively. More importantly, an extremely high level (more than 100 per 10^8 bases) of these DNA adducts was observed in several cases. The level of 4-OHE-derived BεdC was highly correlated with that of HεdC ($R^2 = 0.94$), although BεdC was present at about a 7-fold lower concentration than HεdC. These results suggest that 4-ONE- and 4-OHE-derived DNA adducts are likely to be significant DNA adducts in human tissues, with potential for deleterious effects on human health.

Introduction

Lipid peroxidation (LPO[1]) is a major source of DNA-damaging agents. Decomposition products generated from the LPO of polyunsaturated fatty acids (PUFAs) are highly DNA-reactive, including acrolein, crotonaldehyde, malondialdehyde, and other α,β-unsaturated aldehydes (*1–3*). These electrophilic aldehydes may modify nucleic acid bases to form DNA adducts implicated in mutagenesis, carcinogenesis, accelerated aging, or neurological deterioration (*4–6*). Thus, investigation into the levels and tissue distributions of LPO-derived DNA adducts in humans is important to further understand their possible impact on human health.

LPO-related DNA adducts identified in human tissues are mainly exocyclic etheno and propano adducts such as 1,N^6-etheno-2′-deoxyadenosine (εdA); 3,N^4-etheno-2′-deoxycytidine (εdC); 1, N^2-propano-2′-deoxyguanosines generated from acrolein, crotonaldehyde, and 4-hydroxy-2(*E*)-nonenal (4-HNE); and malondialdehyde-derived 3-(2-deoxy-β-D-erythro-pentofuranosyl)pyrimido[1,2-α]purin-10(3*H*)-one (*7–9*). The long-chain aldehyde 4-HNE is an ω-6 PUFA-peroxidation product that reacts with DNA and protein (*10–12*); furthermore, 4-HNE-related DNA adducts have been reported to be associated with carcinogenesis and Alzheimer's disease (*13–15*). 4-Oxo-2(*E*)-nonenal (4-ONE), another decomposition product of ω-6 PUFAs, has also been shown to induce the formation of etheno DNA adducts carrying aliphatic side chains both in cells and in mouse models, including heptanone-etheno-2′-deoxycytidine (HεdC), heptanone-etheno-2′-deoxyguanosine (HεdG), and heptanone-etheno-2′-deoxyadenosine (HεdA) (*16–18*). 4-Oxo-2(*E*)-hexenal (4-OHE), an ω-3 PUFA-peroxidation product having a chemical structure similar to that of 4-ONE, was recently reported to be able to produce etheno DNA adducts as well,

* Corresponding author. (H.S. (for medical questions)) E-mail: hsugimur@hama-med.ac.jp. (T.M. (for DNA adduct analysis)) E-mail: matsuda@z05.mbox.media.kyoto-u.ac.jp.
[†] Kyoto University.
[‡] National Cheng Kung University.
[§] Hamamatsu University School of Medicine.
[∥] University of Occupational and Environmental Health.

[1] Abbreviations: PUFA, polyunsaturated fatty acid; LPO, lipid peroxidation; 4-HNE, 4-hydroxy-2(*E*)-nonenal; 4-ONE, 4-oxo-2(*E*)-nonenal; 4-OHE, 4-oxo-2(*E*)-hexenal; HεdC, heptanone-etheno-2′-deoxycytidine; HεdG, heptanone-etheno-2′-deoxyguanosine; HεdA, heptanone-etheno-2′-deoxyadenosine; BεdC, butanone-etheno-2′-deoxycytidine; BεmedC, butanone-etheno-2′-deoxy-5-methylcytidine; BεdG, butanone-etheno-2′-deoxyguanosine; BεdA, butanone-etheno-2′-deoxyadenosine; 8-oxodG, 8-oxo-7,8-dihydro-2′-deoxyguanosine; εdA, 1,N^6-etheno-2′-deoxyadenosine; 8-OH-AdG, 8-hydroxy-1,N^2-propanodeoxyguanosine; CdG_2, α-*R*-methyl-γ-hydroxy-1,N^2-propano-2′-deoxyguanosine;COX-2, cyclooxygenase-2; HPNE, 4-hydroperoxy-2(*E*)-nonenal; EDE, 4,5-epoxy-2(*E*)-decenal; 5-LO, 5-lipoxygenase.

10.1021/tx100047d
Published on Web 07/23/2010

such as butanone-etheno-2′-deoxycytidine (BεdC), butanone-etheno-2′-deoxy-5-methyl-cytidine (BεmedC), butanone-etheno-2′-deoxyguanosine (BεdG) (*19–21*), and butanone-etheno-2′-deoxyadenosine (BεdA) (*22*). The levels of 4-ONE- and 4-OHE-related DNA adducts in humans are currently unknown because such adducts were discovered only very recently.

In addition to LPO-derived DNA adducts, various other types of DNA lesions are frequently formed in humans as a consequence of exposure to environmental carcinogens or endogenous DNA-reactive agents. Because a variety of DNA adducts are present in human tissues, comprehensive investigation of these base modifications is necessary to identify the ones most critical to mutagenesis and carcinogenesis in humans. Recently, we developed a novel technique to detect multiple known or unknown DNA adducts simultaneously by using LC-MS/MS (*23, 24*). This approach, named the DNA adductome approach, monitors the neutral loss of 2′-deoxyribose from positively ionized 2′-deoxynucleoside adducts over a certain range of transitions. A variety of DNA adducts detected in DNA samples can be presented and compared by creating an adductome map showing LC retention time, mass-to-charge ratio (*m/z*), and relative peak intensity of each potential DNA adduct. In this study, we applied the DNA adductome approach to several human pulmonary DNA specimens and identified major DNA adducts on the adductome maps. Interestingly, 4-ONE- and 4-OHE-related DNA adducts were found to be major adducts in at least one pulmonary DNA sample, and they were also detected in other DNA samples. We also analyzed the levels of 4-ONE- and 4-OHE-related DNA adducts in various organs of different individuals by using LC-MS/MS. The lesions were found to be widely distributed, with some being present in significant amounts, suggesting that they could be important causative factors in human disease.

Experimental Procedures

Human Autopsy Tissues. Human autopsy tissue samples were collected at Hamamatsu University School of Medicine, Japan, and the study design was approved by the Institutional Review Board of Hamamatsu University School of Medicine (18−4). Sixty-eight samples were obtained from organs of 26 deceased persons, including the colon ($n = 6$), liver ($n = 19$), lung ($n = 12$), pancreas ($n = 9$), spleen ($n = 9$), kidney ($n = 9$), heart ($n = 2$), and small intestine ($n = 2$). The samples were taken within 24 h after death and frozen at −80 °C until DNA extraction. The ages of the subjects (17 males and 9 females) ranged from 26 to 90. Seventeen of them had malignancies as backgrounds, and final remarkable circulatory failures (shock, massive hemorrhage, and sepsis) were validated both clinically and pathologically in 6 cases. Detailed properties of the patients are listed in Supporting Information, Table S-1.

DNA Adduct Standards and Stable Isotope Standards. 4-ONE- and 4-OHE-related DNA adducts (HεdC, HεdA, HεdG, BεdC, BεmedC, BεdA, and BεdG) were synthesized according to previously published methods (*16–20*). The stereoisomers α-*S*- and α-*R*-methyl-γ-hydroxy-1,N^2-propano-2′-deoxyguanosine (CdG_1, CdG_2), 8-hydroxy-1,N^2-propanodeoxyguanosine (8-OH-AdG), and the two stereoisomers of 6-hydroxy-1,N^2-propanodeoxyguanosine (6-OH-AdG_1 and 6-OH-AdG_2) were prepared as previously described (*24*). 8-OxodG and εdA were obtained from Sigma Aldrich Japan (Japan). [U-$^{15}N_5$]-8-oxodG was kindly provided by Dr. Shinya Shibutani, State University of New York, Stony Brook, NY, [$^{15}N_5$, $^{13}C_{10}$]-2-(2′-deoxyguanosine-8-yl)-3-aminobenzanthrone ([$^{15}N_5$, $^{13}C_{10}$]-C8-C2-ABA) was kindly provided by Dr. Takeji Takamura, Kanagawa Institute of Technology, Japan, and other DNA adduct stable isotope standards were synthesized according to previously described methods using [U-$^{15}N_5$]- or [U-$^{15}N_3$]-deoxynucleosides purchased from Cambridge Isotope Laboratories (Andover, MA).

DNA Purification and Hydrolysis. Genomic DNA was isolated and purified from human autopsy samples by using a Gentra Puregene Tissue Kit (QIAGEN, Valencia, CA). DNA extraction was undertaken according to the protocol provided by the manufacturer, with the addition of desferroxamine to all solutions to a final concentration of 0.1 mM.

For DNA adductome analysis, isolated DNA was enzymatically digested as follows: each DNA sample (100 μg) was mixed with 54 μL of digestion buffer (17 mM sodium succinate and 8 mM calcium chloride, pH 6.0) containing 67.5 units of micrococcal nuclease (Worthington, Lakewood, NJ) and 0.255 units of spleen phosphodiesterase (Worthington, Lakewood, NJ). After 3 h of incubation at 37 °C, 3 units of alkaline phosphatase (Sigma-Aldrich, St. Louis, MO), 30 μL of 0.5 M Tris-HCl (pH 8.5), 15 μL of 20 mM zinc sulfate, and 101 μL of Milli-Q water were added, and the mixture were incubated for another 3 h at 37 °C. After this incubation, the mixture was concentrated to 10−20 μL by a Speed-Vac concentrator, and 100 μL of methanol was added to precipitate the protein. After centrifugation, the methanol fraction (supernatant) was transferred to a new Eppendorf tube. The precipitate was extracted with 100 μL of methanol, and the methanol fractions were combined and evaporated to dryness.

For adduct quantification analysis, the DNA sample (50 μg) was mixed with 18 μL of digestion buffer (17 mM sodium succinate and 8 mM calcium chloride, pH 6.0) containing 22.5 units of micrococcal nuclease (Worthington, Lakewood, NJ) and 0.075 units of spleen phosphodiesterase (Worthington, Lakewood, NJ) and 10 units of stable isotope-labeled DNA adduct internal standards mix, including 27.8 nM [U-$^{15}N_5$]-8-oxodG, and 1.1 nM [U-$^{15}N_5$]-εdA, [U-$^{15}N_5$]-CdG_1, [U-$^{15}N_5$]-CdG_2, [U-$^{15}N_5$]-8-OH-AdG, [U-$^{15}N_3$]-HεdC, [U-$^{15}N_5$]-HεdA, [U-$^{15}N_5$]-HεdG, [U-$^{15}N_3$]-BεdC, and [U-$^{15}N_5$]-BεdA. After 3 h of incubation at 37 °C, 3 units of alkaline phosphatase (Sigma-Aldrich, St. Louis, MO), 10 μL of 0.5 M Tris-HCl (pH 8.5), 5 μL of 20 mM zinc sulfate, and 67 μL of Milli-Q water were added, and the mixture were incubated for another 3 h at 37 °C. After this incubation, the mixture was concentrated to 10−20 μL by a Speed-Vac concentrator, and 100 μL of methanol was added to precipitate the protein. After centrifugation, the methanol fraction (supernatant) was transferred to a new Eppendorf tube. The precipitate was extracted with 100 μL of methanol, and the methanol fractions were combined and evaporated to dryness.

DNA Adductome Analysis. Digested DNA used for adductome analysis was redissolved in 120 μL of 30% dimethyl sulfoxide containing 23 nM [$^{15}N_5$, $^{13}C_{10}$]-C8-C2-ABA as the internal standard and then subjected to DNA adductome analysis similar to that described by Kanaly et al. (*24*). Briefly, adductome analysis was carried out using a Quattro Ultima Pt triple stage quadrupole mass spectrometer (Waters-Micromass, Milford, MA) equipped with a Shimadzu LC system (Shimadzu, Japan). An aliquot of digested DNA sample (10 μL) was injected and separated by a Shim-pack XR-ODS column (3.0 mm × 75 mm, Shimadzu, Japan). The column was eluted in a linear gradient of 5% to 80% methanol in water from 0 to 40 min and kept in 80% methanol in water from 40 to 45 min at a flow rate of 0.2 mL/min. Multi-reaction monitoring (MRM) was performed in positive ion mode using nitrogen as the nebulizing gas. Experimental conditions were set as follows: ion source temperature, 130 °C; desolvation temperature, 380 °C; cone voltage, 35 V; collision energy, 15 eV; desolvation gas flow rate, 700 L/h; cone gas flow rate, 35 L/h; collision gas, argon. The strategy was designed to detect the neutral loss of 2′-deoxyribose from positively ionized 2′-deoxynucleoside adducts by monitoring the samples transmitting their $[M + H]^+ \rightarrow [M + H - 116]^+$ transitions. For each DNA sample, 241 MRM transitions were monitored over the *m/z* range from transition *m/z* 250 → 134 to transition 492 → 376. For each sample injection, a total of 31 channels were monitored simultaneously with one channel for each injection reserved to monitor the internal standard [$^{15}N_5$, $^{13}C_{10}$]-C8-C2-ABA at transition *m/z* 526 → 405. Each sample was injected 8 times to complete the monitoring of 241 MRM transitions. Transitions of normal deoxynucleosides, including 252 → 136 ([dA

+ H]$^+$) and 268 → 152 ([dG + H]$^+$), were not monitored in the adductome analysis.

Relative peak intensity of each potential DNA adduct was calculated as follows: (the peak area of the potential DNA adduct)/(the peak area of the internal standard)/(the amount of 2′-deoxyguanosine (dG)). The amount of dG in each DNA sample was estimated by monitoring the dG peak area at 254 nm using the Shimazu SPD-10Avp UV−visible detector connected in series with the LC/MS/MS. The relative peak intensity was plotted as a bubble chart in which the horizontal axis was retention time and the vertical axis is *m/z*. Sodium and potassium adducts of normal deoxynucleosides or other corresponding peaks, such as those detected in the retention times of 9.3−9.5 min (dC), 10.2−10.4 min (dG), 11.2−11.4 min (dT), and 14.0−14.2 min (dA), were not included in the plot.

DNA Adduct Quantification. The digested DNA sample used for quantification was resuspended in 50 μL of 30% dimethyl sulfoxide before LC-MS/MS analysis. An aliquot (20 μL) was injected and separated by the Shim-pack XR-ODS column, eluted in a linear gradient of 5% to 30% methanol in water from 0 to 27 min, 30% to 80% from 27 to 35 min, then kept in 80% from 35 to 40 min at a flow rate of 0.2 mL/min. For the quantification of 4-ONE-derived DNA adducts, HεdC, HεdG, and HεdA, another HPLC-gradient condition was employed because of the high hydrophobicity of these compounds. A remaining aliquot (20 μL) was injected and separated by the same column, eluted in a linear gradient of 45% to 90% methanol in water from 0 to 20 min at a flow rate of 0.2 mL/min. Experimental conditions were identical to those set for adductome analysis except that the cone voltage and collision energy were different for different DNA adducts. The collision energies and characteristic reactions monitored for the different DNA adducts are as follows (cone voltage (V), collision energy (eV), base ionS → product ion): [U-$^{15}N_5$]-8-oxodG (40, 12, 288.8 → 172.8), [U-$^{15}N_5$]-εdA (35, 14, 280.9 → 164.9), [U-$^{15}N_5$]-CdG_1 and [U-$^{15}N_5$]-CdG_2 (35, 10, 343.0 → 227.0), [U-$^{15}N_5$]-8-OH-AdG (35, 10, 329.3 → 213.3), [U-$^{15}N_3$]-HεdC (35, 10, 367.0 → 251.0), [U-$^{15}N_5$]-HεdA (35, 10, 393.0 → 277.0), [U-$^{15}N_5$]-HεdG (35, 10, 409.0 → 293.0), [U-$^{15}N_3$]-BεdC (35, 10, 324.8 → 208.6), and [U-$^{15}N_5$]-BεdA (35, 10, 351.0 → 234.8), 8-oxodG (40, 12, 283.8 → 167.8), εdA (35, 14, 275.9 → 159.9), CdG_1 and CdG_2 (35, 10, 338.0 → 222.0), 8-OH-AdG, 6-OH-AdG_1, and 6-OH-AdG_2 (35, 10, 324.3 → 208.3), HεdC (35, 10, 364.0 → 248.0), HεdA (35, 10, 388.0 → 272.0), HεdG (35, 10, 404.0 → 288.0), BεdC (35, 10, 321.8 → 205.6), BεmedC (35, 20, 335.9 → 220.0), and BεdA (35, 10, 351.0 → 234.8) and BεdG (35, 20, 362.0 → 245.9).

The amount of each DNA adduct was quantified by calculating the peak area ratio of the target DNA adduct and its specific internal standard ([U-$^{15}N_3$]-BεdC was used for BεdC and BεmedC, and [U-$^{15}N_5$]-BεdA was used for BεdA and BεdG). Calibration curves were obtained by using authentic standards spiked with isotope internal standards. The concentration of dG in each DNA sample was also monitored as described in the DNA Adductome Analysis section. The number of DNA adducts per 10^8 bases was calculated by the following equation: number of DNA adducts per 10^8 bases = adduct level (fmol/μmol dG) × 0.218(μmol dG/μmol dN) × 10^{-1}, as described previously (*25*).

Results

Adductome Analysis of DNA Extracted from Human Lung Autopsy Tissues. We applied adductome analysis to DNA extracted from four human lung autopsy samples to simultaneously detect a variety of known and unknown DNA adducts in human pulmonary DNA. Although adductome analysis is semiquantitative, this analysis would help to grasp a complete picture of the DNA adducts in human samples. Several peaks were identified as corresponding to known DNA adducts by showing identical *m/z* and LC retention times to DNA adduct standards. Figure 1 shows the adductome maps of two human pulmonary DNA samples having different patterns of DNA

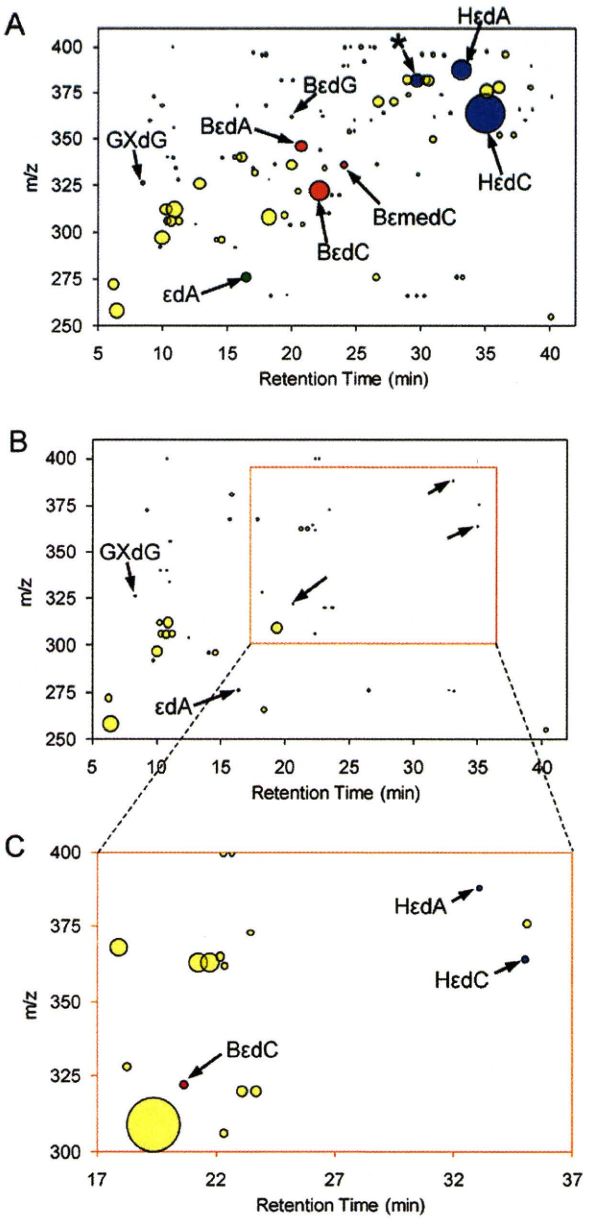

Figure 1. A and B show the DNA adductome maps of two human pulmonary DNA samples from different individuals, and C is a close-up of a selected area in B. Each circle represents one DNA adduct candidate detected by adductome analysis using LC-MS/MS. HPLC retention time, mass to charge ratio (*m/z*), and relative intensity (shown by the size of each circle, which is proportional to the peak area of each DNA adduct candidate divided by the peak area of the internal standard and the amount of 2′-deoxyguanosine) of each DNA adduct candidate can be found on the maps. Blue circles represent corresponding peaks of 4-ONE-related DNA adducts, while orange circles represent 4-OHE-related DNA adducts. Green circles are the other lipid-peroxidation derived DNA adducts, and yellow circles represent unidentified peaks. GXdG: 1,N^2-glyoxyal-dG. *: heptanone-ethano-2′-deoxycytidine.

adduct composition. Numerous DNA adducts can be seen in Figure 1A, and LPO-induced DNA adducts were detected as major peaks, including HεdC, HεdA, BεdC, BεdA, BεmedC, BεdG, εdA, and 1,N^2-glyoxal-dG. Although fewer DNA adducts were found in the sample represented in Figure 1B, LPO-induced DNA adducts derived from 4-ONE and 4-OHE (i.e., HεdC, HεdA, and BεdC) were nonetheless detected. Adductome maps of two other human pulmonary DNA samples have patterns similar to that shown in Figure 1B (data not shown),